

## Mechanism of Thermal Transport in Dilute Nanocolloids

Jacob Eapen,<sup>1</sup> Ju Li,<sup>2</sup> and Sidney Yip<sup>1,3</sup>

<sup>1</sup>Department of Nuclear Science and Engineering, Massachusetts Institute of Technology, Cambridge, Massachusetts 02139, USA

<sup>2</sup>Department of Materials Science and Engineering, Ohio State University, Columbus, Ohio 43210, USA

<sup>3</sup>Department of Materials Science and Engineering, Massachusetts Institute of Technology, Cambridge, Massachusetts 02139, USA

(Received 27 April 2006; published 10 January 2007)

Thermal conduction modes in a nanocolloid (nanofluid) are quantitatively assessed by combining linear response theory with molecular dynamics simulations. The microscopic heat flux is decomposed into three additive fluctuation modes, namely, kinetic, potential, and collision. For low volume fractions (<1%) of nanosized platinum clusters which interact strongly with xenon host liquid, a significant thermal conductivity enhancement results from the self correlation in the potential flux. Our findings reveal a molecular-level mechanism for enhanced thermal conductivity in nanocolloids with short-ranged attraction and offer predictions that can be experimentally tested.

DOI: 10.1103/PhysRevLett.98.028302

PACS numbers: 47.57.J-, 65.20.+w, 66.60.+a

Recent thermal conductivity measurements on dispersions of metallic and oxide clusters have stimulated interests in the thermal transport mechanisms of colloidal systems at the nanoscale [1–4]. At variance with the classical effective-medium theories [5], where the colloidal system is homogenized as a single cluster in the host fluid, unusually large (18%–40%) thermal conductivity enhancements at very low volume fractions (0.2%–0.6%) are reported with (10 nm) copper and iron clusters in ethylene glycol [3,4,6]. Equally puzzling is the thermal conductivity behavior with (11–150 nm) metallic oxide nanoclusters (Al<sub>2</sub>O<sub>3</sub>, CuO, Fe<sub>3</sub>O<sub>4</sub>, TiO<sub>2</sub>) in water such as the cluster size dependency [2], saturation at higher volume fractions [7,8], and the lack of correlation to the intrinsic thermal conductivity of the clusters [8]. Attempts have been made to attribute these characteristics to the Brownian motion of the clusters [9], or to a phenomenological microconvection mechanism [10,11]. Order of magnitude analyses [12,13] and a molecular dynamics (MD) simulation [14] however, show these effects do not contribute significantly to the thermal conductivity. Solidlike layering of the host molecules around the nanoclusters is also proposed as an enhancement mechanism [15] but the results from a MD simulation [16] do not support this hypothesis. Furthermore, the mismatch of vibrational frequencies at the cluster-fluid interface [17] suggests a decrease in the thermal conductivity. More recently, it is shown with a three level homogenization that a linear chainlike cluster agglomeration can augment the thermal conductivity of a colloid [18]. While this model may explain the saturation behavior observed at higher volume fractions, the lack of correlation to the cluster thermal conductivity [3,8] could suggest a different mechanism. Given the lack of consensus, a statistical mechanical study that does not postulate the mechanisms, *a priori*, is needed to clarify the theoretical implications of this phenomenon.

Linear response theory (Green-Kubo formalism), in conjunction with molecular dynamics simulations, provides quantitative means for analyzing thermal conduction in colloidal fluids. We apply this established approach to a xenon-platinum nanocolloidal model to decompose the dynamical thermal conductivity in terms of self and cross correlations of the three modes that make up the microscopic heat flux vector, namely, the kinetic, the potential, and the collision. In this manner, we are able to examine the interplay between the molecular mechanisms that govern the variation of the thermal conductivity with volume fraction. For the specific case of subnanometer clusters of Pt atoms in a host fluid Xe, we find conductivity enhancements up to 35% relative to the pure fluid with a cluster concentration below 1%. This effect is caused by the self correlation of the potential flux which arises from the strong Xe-Pt cross interaction.

In the linear response theory, the thermal conductivity is calculated as the time integral of the heat flux autocorrelation function [19] as given by (1)

$$\lambda = \frac{1}{3Vk_B T^2} \int_0^\infty \langle \mathbf{J}_q(\tau) \mathbf{J}_q(0) \rangle d\tau, \quad (1)$$

where  $\mathbf{J}_q$  is the instantaneous microscopic heat flux vector

$$\mathbf{J}_q = \frac{d}{dt} \sum_{i=1}^N \mathbf{r}_i \tilde{E}_i, \quad (2)$$

with  $\tilde{E}_i$  denoting the excess energy,  $\tilde{E}_i = E_i - \langle E_i \rangle$ . For a two-component system [20], one has the following form in (3) which shows the three modes, the kinetic (*K*), the potential (*P*), and collision (*C*) that constitute the heat flux. In this expression  $\alpha$  and  $\beta$  denote Xe and Pt, and  $h$  stands for the mean partial enthalpy which is calculated as the sum of the average kinetic energy, potential energy and

collision. Thus, the three modes  $K$ ,  $P$ , and  $C$  now correspond to the fluctuations in the heat flux. Strictly speaking (3) is valid only for a homogeneous system [21] where density gradients are negligible. To validate our assumption, we have calculated the heat flux directly from a nonequilibrium molecular dynamics simulation (NEMD) [22] and find that the heat flux determined by this method agrees with the time average of (3) to within 5% or better. The small molecular dimensions in relation to the system size explain the good agreement observed in this simulation [23].

$$\mathbf{J}_q = \sum_{k=\alpha}^{\beta} \sum_{i=1}^{N_k} \frac{1}{2} \overbrace{m_i^k (v_i^k)^2}^K \mathbf{v}_i^k + \sum_{k=\alpha}^{\beta} \sum_{l=\alpha}^{\beta} \sum_{i=1}^{N_k} \sum_{j>i}^{N_l} \left[ \overbrace{\mathbf{I}U(r_{ij}^{kl})}^P - \overbrace{\mathbf{r}_{ij}^{kl} \otimes \frac{\partial U(r_{ij}^{kl})}{\partial \mathbf{r}_{ij}^{kl}}}_C \right] \cdot \mathbf{v}_i^k - \sum_{k=\alpha}^{\beta} h^k \sum_{i=1}^{N_k} \mathbf{v}_i^k. \quad (3)$$

The model system we analyze consists of monodispersed, subnanometer clusters of Pt atoms in liquid Xe. All interatomic interactions are taken to be of the Lennard-Jones (LJ) form, with parameters  $\varepsilon_{\text{Xe-Xe}} = 1.977$  kJ/mol and  $\sigma_{\text{Xe-Xe}} = 3.95$  Å [24],  $\varepsilon_{\text{Xe-Pt}} = 24.047$  kJ/mol and  $\sigma_{\text{Xe-Pt}} = 2.732$  Å [25], and  $\varepsilon_{\text{Pt-Pt}} = 65.77$  kJ/mol and  $\sigma_{\text{Pt-Pt}} = 2.54$  Å [26]. The Xe-Pt potential in [25] is fitted to a variety of scattering data and thermodynamic properties, and has a deeper attractive potential than what is estimated with the classical Lorentz-Berthelot mixing rule [20]. As shown later, the Pt-Pt interaction, evidently the strongest in the system, has only a minor role in the conduction mechanisms while the cross interaction between Xe and Pt, the next strongest, plays a dominant role.

For the MD simulations, geometrically similar clusters, each consisting of 10 atoms, are dispersed randomly in the base fluid. All the simulations are performed in a periodic cube of 2048 atoms. The nanocolloid is equilibrated at 200 K and 0 atms using the Berendsen barostat and velocity rescaling. To ensure the clusters do not agglomerate, a repulsion potential  $U_R(r_{ij}) = A(1 - r_{ij}/r_c)^2$  is introduced between the clusters, with  $A$ , an arbitrary constant (49.43 kJ/mol) and  $r_c$ , a cutoff radius (17.78 Å). Once the equilibration is attained, the heat flux autocorrelation function (HACF) is then averaged over 2000 sets in the  $NVE$  ensemble. Each transport coefficient is further averaged over 12 independent runs for additional phase-space sampling. The volume fraction ( $\phi$ ) is calculated as  $\pi n \rho a_{\text{Pt}}^3 / 6\nu$ , where  $n$  is the Pt number fraction,  $\rho$ , the number density and  $a_{\text{Pt}}$ , the relative nearest neighbor distance in Pt. The fcc packing fraction  $\nu$ , assigns the void inside the cluster to the cluster volume. A nanocluster number fraction of 80/2048 thus, corresponds to  $\phi = 0.8\%$ .

Figure 1 shows the variation of the overall thermal conductivity  $\lambda$  with volume fraction  $\phi$  over the range 0%–0.8%. Since the heat flux is a sum of three modes ( $K$ ,  $P$ , and  $C$ ), the conductivity can be expressed as a sum of nine terms which can be conveniently grouped together into self correlations,  $KK$ ,  $PP$ , and  $CC$  and cross correlations  $PC$ ,  $PK$ , etc. Moreover, each component is a sum over atom species, Xe-Xe, Xe-Pt, and Pt-Pt. The first noteworthy result in Fig. 1 is the conductivity for the pure fluid ( $\phi = 0$ ) which has a dominant contribution of about 90% from  $CC + PC + CP(\text{Xe-Xe})$  with 75% coming from  $CC(\text{Xe-Xe})$  and the remaining 15% from  $PC +$

$CP(\text{Xe-Xe})$ . The  $KK(\text{Xe-Xe})$  and  $PP(\text{Xe-Xe})$  contributions are negligible and the cross terms account for the remaining 10%. For finite volume fractions, the sum of the  $CC$ ,  $PC$ , and  $CP$  correlations remains more or less constant except at higher volume fractions. This implies that the contributions of  $CC + PC + CP(\text{Xe-Xe})$  and  $CC + PC + CP(\text{Pt-Pt})$  correlations are relatively small. Meanwhile, the total thermal conductivity ( $\lambda$ ) shows an increase which is significantly higher than the prediction of the Maxwell's effective-medium theory [5]. This enhancement primarily comes from the increase in the  $PP$  correlation. In contrast, the  $KK$  correlation is practically zero for all volume fractions.

We will look into the physical origin of the various correlations. The  $KK$  correlation is dominant only for dilute gases with relatively weak interatomic forces. The negligible  $KK$  correlation indicates that the Brownian motion of the clusters has only an insignificant role in the enhancement, a result also obtained by previous analyses [12–14]). The  $CC$  correlation involves the virial interaction or the work done by the interatomic forces and in perfect crystals, it represents the vibrational or phonon modes [27]. As demonstrated before, this term contributes most to the thermal conductivity in typical liquids. The most remarkable aspect in Fig. 1 is the increase of  $PP$

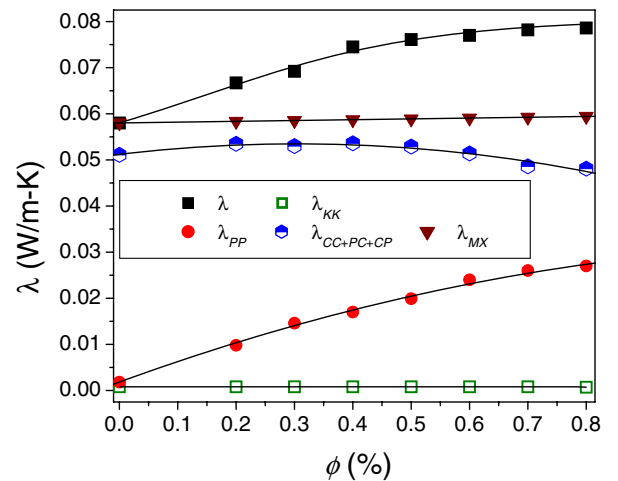


FIG. 1 (color online). Thermal conductivity of the Xe-Pt nanocolloid system and the contributions from  $KK$ ,  $PP$ , and  $CC + PC + CP$  correlations. The prediction of Maxwell's effective-medium theory is denoted by  $\lambda_{\text{MX}}$ .

correlation. To our knowledge, this is an unusual mode of energy transport which is typically insignificant in a single component system. We have verified through MD simulations the negligible contribution of  $PP$  correlation for Ar in the solid state ( $<1\%$ ) and the liquid state ( $<4\%$ ). Furthermore, the effect is also seen to be insignificant in binary noble gas liquid systems ( $<4\%$ ).

We will now study the  $PP$  correlation function to find its physical origin. Figure 2(b) depicts how  $PP$  correlation, which is responsible for the conductivity enhancement, varies with increasing volume fraction. One sees the onset of pronounced oscillations with increasing volume fraction. Three characteristic peaks appear in the Fourier transform (power spectra) of the correlation function [Fig. 2(a)]. The frequency of each peak matches well with the estimate using the curvature of the potential well,  $\sqrt{(\partial^2 U / \partial^2 r)|_{r=r_{eq}} / 4\pi^2 m}$ , for the Xe-Xe, Xe-Pt, and Pt-Pt interactions, respectively. The frequency estimate from the above curvature corresponds to that of a harmonic vibration about the energy minima. The much stronger Xe-Pt peak intensity shows that the conductivity enhancement arises from the  $PP(\text{Xe-Pt})$  correlation while the  $PP(\text{Pt-Pt})$  and  $PP(\text{Xe-Xe})$  correlations are relatively insignificant.

To study the spatial nature of Xe-Pt interactions, we select five representative Xe atoms from the first coordination shell of a platinum cluster, and follow the temporal behavior in the kinetic ( $T$ ) and potential ( $U$ ) energies of these atoms, keeping in mind that all the five atoms are structurally equivalent in every way. We then calculate the dynamic fluctuation amplitude  $\Lambda$  defined as the standard deviation in the kinetic or potential energies of each atom, averaged over all the like atoms. For example,  $\Lambda^U$  of the Pt atoms is defined as the standard deviation of the potential energy of each Pt atom averaged over all Pt atoms. The data shown in Fig. 3 are taken from the final 77 ps of a single run ( $\phi = 0.8\%$ ) over which the relative change in the total energy is less than 0.001%. The Xe atoms in close vicinity to the Pt atoms experience large potential energy fluctuations without a concomitant change in the kinetic energy as shown in Fig. 3(a) and 3(b). Several fluid atoms have varying levels of potential energy with some atoms

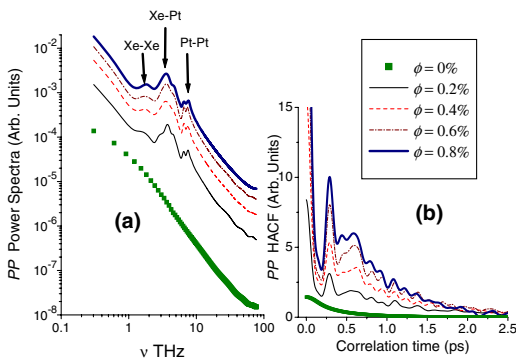


FIG. 2 (color online). (a) Power spectra. (b) Potential-potential ( $PP$ ) heat flux autocorrelation function.

displaying large fluctuations without a noticeable change in their average values (e.g., atom  $A$ ). A smaller set of fluid atoms show pronounced jumps from one energy level to another (e.g., atom  $B$ ) which happens when the fluid atom gets trapped in the potential cage formed by the solid atoms and vice versa. Interestingly, a local cooperativity can be seen in the concerted jumps in  $U(C)$ ,  $U(D)$  and  $U(E)$  without a noticeable change in the kinetic energy [see  $T(E)$ ] or total energy. This pronounced cooperative exchange thus provides a mechanism for additional energy transfer.

Figure 3(c) depicts the dynamic fluctuation amplitudes,  $\Lambda^T$  and  $\Lambda^U$ , of the fluids atoms placed in different radial shells around the nanoclusters. In the first shell located at 3.16 Å from the cluster,  $\Lambda^U$  is 53% higher than  $\Lambda^T$ . As expected,  $\Lambda^U$  approaches the bulk value away from the nanoclusters. This reinforces the view that the potential energy is cooperatively transferred among the Xe atoms in close proximity [O(1 nm)] to the platinum atoms and indicates the presence of a dynamic interface shell around the nanoclusters. To remove the empiricism of arbitrarily assigning a shell thickness, we calculate the *excess*  $\Lambda^U$  of the Xe atoms in a nanocolloid simulation relative to  $\Lambda^U$  of the Xe atoms in the base fluid simulation. The enhancement in  $\lambda$  is seen to be linearly correlated to the excess fluctuations in the Xe atoms as shown in Fig. 3(d), except at higher volume fractions ( $\phi \geq 0.5$ ) where there is a reduction in the contribution from the  $CC + PC + CP$  correlation (see Fig. 1).

In conclusion, we have shown using linear response theory that the thermal conductivity enhancements in a Xe-Pt nanocolloid system arise from a strong cluster-fluid

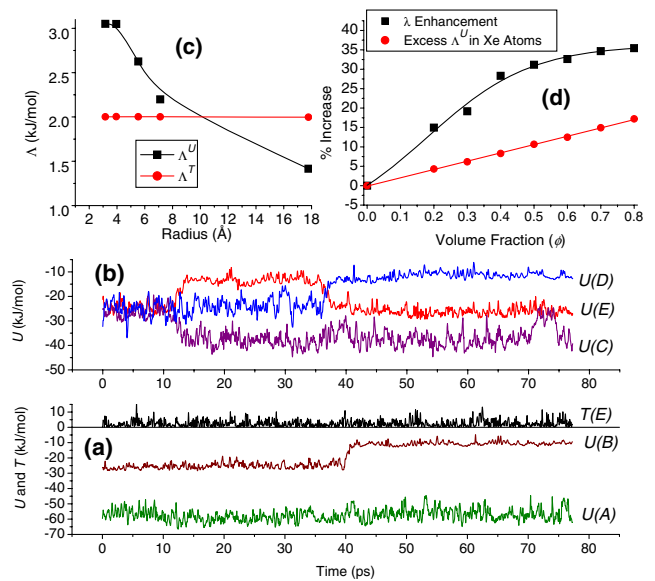


FIG. 3 (color online). (a) and (b) Potential ( $U$ ) and kinetic ( $K$ ) energy fluctuations in a few representative Xe atoms surrounding a Pt cluster. (c) Dynamic fluctuation amplitude  $\Lambda^U$  and  $\Lambda^T$  in Xe atoms for different radial shells around the Pt clusters. (d) Excess  $\Lambda^U$  of the Xe atoms and the enhancement in  $\lambda$ .

attraction through the self correlation of the potential flux ( $PP$ ). Our work highlights the significance of surface interactions and characterizes the thermal conductivity enhancement primarily as a surface phenomenon. The interfacial fluid atoms form a dynamic layer around the nanoclusters where potential energy is cooperatively exchanged. In a future publication, we will show the correlation between the interfacial structure and dynamics, and how the dynamic interfacial layers form a percolating network which assists in transferring the excess potential energy fluctuations.

We believe that the mechanisms which we have identified are applicable to a broader class of nanocolloids. For example, we anticipate little or moderate thermal conductivity enhancements from the proposed mechanism in gaseous nanocolloids because of small potential energies, and colloids with lyophobic clusters such as diamond and carbon fullerenes due to strong cluster-fluid repulsion. Our theory offers possible avenues for optimizing the nanocolloids by developing clusters that have functionalized surface layers to maximize the attraction with the fluid molecules.

We acknowledge useful discussions with P. Keblinski and J. Buongiorno. The work of J. E. and S. Y. is supported by the National Science Foundation under Grant No. 0205411, with computational support via Grant No. IMR-0414849. The work of J. L. is supported by DOE Basic Energy Sciences DE-FG02-06ER46330 and the Ohio Supercomputer Center.

- 
- [1] S. K. Das *et al.*, *J. Heat Transfer* **125**, 567 (2003).
  - [2] C. H. Chon *et al.*, *Appl. Phys. Lett.* **87**, 153107 (2005).
  - [3] T. K. Hong, H. S. Yang, and C. J. Choi, *J. Appl. Phys.* **97**, 064311 (2005).
  - [4] J. A. Eastman *et al.*, *Appl. Phys. Lett.* **78**, 718 (2001).

- [5] K. Markov, L. Preziosi, and G. C. Gaunard, *Heterogeneous Media: Micromechanics Modeling Methods and Simulations* (Birkhauser, Cambridge, MA, 2000).
- [6] K. S. Hong, T. K. Hong, and H. S. Yang, *Appl. Phys. Lett.* **88**, 031901 (2006).
- [7] S. M. S. Murshed, K. C. Leong, and C. Yang, *Int. J. Therm. Sci.* **44**, 367 (2005).
- [8] H. Zhu *et al.*, *Appl. Phys. Lett.* **89**, 023123 (2006).
- [9] D. H. Kumar *et al.*, *Phys. Rev. Lett.* **93**, 144301 (2004).
- [10] S. P. Jang and S. U. S. Choi, *Appl. Phys. Lett.* **84**, 4316 (2004).
- [11] R. Prasher, P. Bhattacharya, and P. E. Phelan, *Phys. Rev. Lett.* **94**, 025901 (2005).
- [12] S. Bastea, *Phys. Rev. Lett.* **95**, 019401 (2005).
- [13] P. Keblinski and D. G. Cahill, *Phys. Rev. Lett.* **95**, 209401 (2005).
- [14] W. Evans, J. Fish, and P. Keblinski, *Appl. Phys. Lett.* **88**, 093116 (2006).
- [15] P. Keblinski *et al.*, *Int. J. Heat Mass Transfer* **45**, 855 (2002).
- [16] L. Xue *et al.*, *Int. J. Heat and Mass Transfer* **47**, 4277 (2004).
- [17] S. Shenogin *et al.*, *J. Appl. Phys.* **95**, 8136 (2004).
- [18] R. Prasher *et al.*, *Appl. Phys. Lett.* **89**, 143119 (2006).
- [19] D. A. McQuarrie, *Statistical Mechanics* (University Science Books, California, 2000).
- [20] C. Hoheisel, *Theoretical Treatment of Liquids and Mixtures* (Elsevier, Amsterdam, 1987).
- [21] B. D. Todd, P. J. Daivis, and D. J. Evans, *Phys. Rev. E* **51**, 4362 (1995).
- [22] F. Müller-Plathe, *J. Chem. Phys.* **106**, 6082 (1997).
- [23] H. J. M. Hanley, *Transport Phenomena in Fluids* (Marcel Dekker, New York, 1969).
- [24] F. F. Abraham, *Phys. Rev. B* **29**, 2606 (1984).
- [25] J. A. Barker and C. T. Rettner, *J. Chem. Phys.* **97**, 5844 (1992).
- [26] S.-B. Zhu and M. R. Philpott, *J. Chem. Phys.* **100**, 6961 (1994).
- [27] S. G. Volz and G. Chen, *Phys. Rev. B* **61**, 2651 (2000).